UNIVERSAL WISER
PUBLISHER

Research Article

Effect of Carboxylate Additives on $CaCO_3$ Particle Size by Precipitation Method Using Scallop Shell

Hideo Maruyama[1]* [ID], Shiro Takahashi[2] [ID]

[1] Division of Marine Biosciences, Graduate School of Fisheries Sciences, Hokkaido University, Minato 3-1-1, Hakodate, Hokkaido 041-8611, Japan
[2] Hokkaido Industrial Technology Center, 379 Kikyo-cho, Hakodate, Hokkaido 041-0801, Japan
 E-mail: maruyama@fish.hokudai.ac.jp

Abstract: The effect of carboxylate on the particle size of $CaCO_3$ derived from scallop shells was investigated. Shell was dissolved in HCl solution and used as a raw material for $CaCO_3$ particles. As the carboxylate additives, tartrate, oxalate, phthalate, and citrate were employed. The average diameter of particles, D_a, was found to be a function of the molar ratio of COO^-/CO_3^{2-}. In the case of adding tartrate and phthalate, D_a was varied as having a local minimum value at the molar ratio of 1–5. In the case of adding oxalate and citrate, D_a was varied as reaching the minimum value at the molar ratio of 1–2. These sizes were about 0.1–0.25 times smaller than those without adding (21 μm). The characterization of the particles was conducted by SEM images and X-ray diffraction patterns. Particles were found to have a crystal structure of calcite, however, in the case of tartrate and phthalate, calcium tartrate tetrahydrate and vaterite were found.

Keywords: calcium carbonate, particle size control, carboxylate, additives, XRD pattern

1. Introduction

Calcium carbonate is one of the most abundant minerals in the world as limestone[1]. Calcium carbonate is widely used in various industries[2]. It is most commonly used as heavy calcium carbonate, which is obtained by grinding limestone, and as light calcium carbonate, which is obtained by precipitation or by venting carbon dioxide into a calcium hydroxide suspension to produce fine calcium carbonate particles[3]. Finer calcium carbonate particles are also in high demand and widely used because they can be used as fillers, which has a wide range of applications including building materials, cement, paper manufacturing, plastics, rubber, food, and pharmaceuticals, and have been used as a hardening agent for brewing water, a deacidifying agent for sake, a neutralizing agent for candy, and mixed with salt in pickled vegetables[4].

On the other hand, in Japan, scallop farming has been one of the major maricultures[5]. For example, the annual production of cultured scallops was ca. three hundred ninety thousand tons in Hokkaido prefecture in 2019, on the other hand, the waste shells were ca. fourteen hundred thousand tons in 2019[6]. The waste scallop shell is usually stacked on the roadside, becoming a serious environmental problem. The useful utilization of waste scallop shells is important to solve the environmental problem[7]. These waste shells can be regarded as an important calcium carbonate resource as well as limestone, and the development of more active utilization methods is very important from the viewpoint of the utilization

of waste resources. We recognize that promoting the utilization of shellfish waste is not only an issue for our region but also a common challenge for all regions of the world with a thriving fishing industry.

In recent years, it has been reported that the particle size of calcium carbonate produced by carbon dioxide aeration [8,9] or liquid-liquid precipitation [10–12] can be controlled by changing the liquid composition [13–15] of the suspension or by adding several additives such as amino acids [16–20], fatty acids [21,22], surfactant [23,24], polymers [25–29], and inorganic additives [30–32]. Among several additives, carboxylate has received particular attention. Sun et al. (2020) used some carboxylic additives (polyacrylic acid, citric acid, adipic acid, 6-aminocaproic acid, 4-aminobutyric acid, and hexanoic acid) to stabilize calcium carbonate and the porosity was remarkably improved [33]. Jia et al. (2022) reported the preparation of small amorphous calcium carbonate clusters in stabilized form using carboxylated hyaluronic acid and carboxylated dextran [34]. Tobler et al. (2015) have monitored amorphous calcium carbonate formation and its crystallization in real-time as a function of citrate concentration in solution [35]. Miyashita et al. (2018) have investigated the influence of low-molecular-weight dicarboxylic acids (oxalic, glutaric, and malonic acids) on the formation of calcium carbonate [36]. Henderson et al. (2008) have manipulated the processes of crystal nucleation and growth of calcium carbonate using the vapor diffusion method by adding water-soluble straight-chain monocarboxylic acids (ethanoic, propanoic, butanoic, and pentanoic acids) [37].

We focused on the liquid precipitation method, which can produce light calcium carbonate relatively easily. According to many reports regarding the generation of amorphous calcium carbonate described above, the assumption has been suggested that if divalent anions, which are the competitors of carbonate ions that bind to calcium ions, were present in the liquid, the binding rate of calcium ions to carbonate ions could be controlled, and as a result, the particle size distribution of calcium carbonate particles could be controlled, and dicarboxylates are one of the suitable substances as the competitors. For the utilization of bioresources, we have already conducted the esterification of lipids using calcined waste seashell (scallop) as a solid base catalysis [38]. In the future, we will consider using calcination of mixtures of pulverized seashells and dicarboxylates, amino acids, and other metal ions as solid base catalysts.

The purpose of this study is to clarify the effect of carboxylate concentration on the size of calcium carbonate particles and the effect of carboxylate concentration on the resulting particle structure from a practical point of view. In this study, experimental investigations were carried out using a calcium solution obtained by dissolving waste shells with a concentrated hydrogen chloride solution. However, we fully expect that this method will be criticized because it releases carbon dioxide from the shells, which is not good for the environment. However, we would like to understand that this is an experiment and research to obtain basic knowledge. For comparison, reagent calcium solutions (mainly aqueous calcium chloride solutions) were also used. In particular, the effect of the molar ratio of carboxyl groups to carbonate ions on the average particle size was investigated, and mobile observation by SEM and XRD provided insight into the calcium carbonate polymorph.

2. Materials and methods

2.1 *Materials*

2.1.1 *Reagents*

Calcium chloride, sodium carbonate, potassium sodium tartrate, potassium hydrogen phthalate, sodium oxalate, sodium citrate, sodium hydroxide, hydrochloric acid, Eriochrome Black T, and Hydroxylammonium chloride were purchased from Fujifilm Wako Pure Chemical Co. (Japan). Sodium ethylene diamine tetraacetate (EDTA-2Na) solution (0.1 mol/L) was purchased from Dojin Chemical (Japan). All purchased reagents were used without further purification.

2.1.2 *Scallop shell*

The scallop shell was obtained from commercial markets or restaurants in Hakodate City, Japan. They were mostly captured at Funka Bay (Hokkaido prefecture) and Mutsu Bay (Aomori prefecture) in Japan.

2.2 Preparation of calcium solution derived from scallop shells

The scallop shell was washed well with tap water and was rinsed with distilled water. They were dried at room temperature for 24 h. The shells were crushed into appropriate size (about 2–3 mm) by using a hammer. 40 g of the crushed shell pieces were taken in a 500 mL glass beaker. Then, 80 mL of HCl solution (11.5 mol/L) was added to the beaker, and the suspension was stirred with a magnetic stirrer at 100 rpm for 24 h to dissolve shell pieces. After dissolving shell pieces with HCl solution, the solution was filtered with a quantitative paper filter (5C) to remove residual shell pieces. By repeating this manner, the dissolved shell solution was collected as the calcium solution derived from scallop shells. Approximately 95% of the shells could be dissolved by this operation. The calcium ion concentration in the dissolution solution was 1.85 mol/L. Hereafter this solution is expressed as a CaSC solution. The calcium concentration of the CaSC solution was determined by titration with EDTA solution and Eriochrome Black T as an indicator. In the experiments, the CaSC solution was used to dilute to the desired concentration.

2.3 Synthesis procedure of calcium carbonate

The calcium carbonate was synthesized by fast precipitation in a glass beaker. In this method, two solutions were mixed to produce $CaCO_3$ particles. The two solutions were the diluted CaSC solution (or $CaCl_2$ solution) and the bicarboxylate/Na_2CO_3 mixed solution, respectively. $CaCl_2$ solution was used as a reagent-derived calcium solution for comparison with CaCS solution. In this study, the calcium ion concentrations of all solutions containing calcium ions used in the precipitation formation experiments were prepared at 0.1 mol/L for the experiments. The bicarboxylate/Na_2CO_3 mixed solution was prepared by dissolving sodium carbonate and dicarboxylate together to achieve the desired molar ratio of carboxyl groups to carbonate ions. The pH value of solutions was measured with a pH meter (520A or 920A, ORION, USA).

150 mL of the diluted CaSC solution was taken in a 500 mL glass beaker and the solution was stirred with a magnetic stirrer at 300 rpm. Then, 150 mL of the bicarboxylate/Na_2CO_3 mixed solution was poured into the 500 mL beaker, and two solutions were mixed well by stirring for 1 h. After this, the particle distribution was measured with a laser scattering size distribution analyzer (LA-300, HORIBA, Ltd., Japan). The particles in the suspension were collected by filtration (5C paper filter) and were rinsed with deionized water. Then, the collected particles on the paper filter were dried in a dryer for 24 h at 70 °C. The particle production by precipitation and measurement of the particle size distribution was conducted at least two times.

2.4 Measurements of particle characterization

The morphology of the collected particles was observed using scanning electron microscopy (SEM, JSM6010LA, JEOL Ltd., Japan). The X-ray diffraction pattern was recorded by an X-ray diffractometer (XRD, MiniFlex, Rigaku Co., Japan). The measurement conditions are as follows: wavelength: Cu Kα radiation at 40 kV and 15 mA, X-ray tube output: 40 kV-200 mA, 2θ: 10 to 80°, speed: 10°/min.

3. Results and discussion

3.1 Particle diameter distribution and influence of initial pH value of the calcium solution

Figure 1 shows the typical result of the measurement of particle diameter distribution. This is an example of the measurement using sodium oxalate as the dicarboxylate. The carbonate ion concentrations in the mixed solution were varied from 0.05, 0.1, and 0.2 M. As the carbonate ion concentration increases, the particle size showing the maximum frequency becomes smaller as the molar ratio decreases. In Figure 1a, the molar ratio is 4, in Figure 1b, the molar ratio is 2, and in Figure 1c, the molar ratio is 0.5, respectively. A similar trend was generally observed when other dicarboxylates were used.

We assumed that the carboxyl functional groups of dicarboxylate in the dissociated state would become competitors of CO_3^{2-} for the binding with Ca^{2+} and that the particle size of $CaCO_3$ could be controlled by reducing the frequency of collisions between Ca^{2+} and CO_3^{2-} and by slowing down the binding rate. The pH value of 0.1 M CaSC solution is about 0.9. When mixing the carbonate solution with the calcium solution, the same volume was mixed, so the dissolved substances were diluted by about half. This might cause the pH of the solution to be too low to dissociate the carboxyl groups of carboxylate. At first, we investigated the influence of the initial pH of the calcium solution on the average diameter, D_a, of the generated particles. The results are shown in Figure 2. The concentrations used in these experiments are as follows: the concentration of Ca^{2+} in the calcium solution was 0.1 M, and the concentration of CO_3^{2-} and carboxylate were also 0.1 M. Several profiles were found with four kinds of carboxylates. At about pH 1, in the case of using oxalate and citrate, D_a became about 1–2 μm, which was the smallest in this experimental range. In the case of tartrate, D_a decreased abruptly from 15 μm to 5 μm. In the range of pH 2–6, D_a was stable at 3–5 μm. The pH of the ca. 18-folds diluted CaSC solution ($[Ca^{2+}]$ = 0.1 mol/L) was pH 1.23. Thus, in almost all experiments, the initial pH of the calcium solution was set to pH 1–1.5.
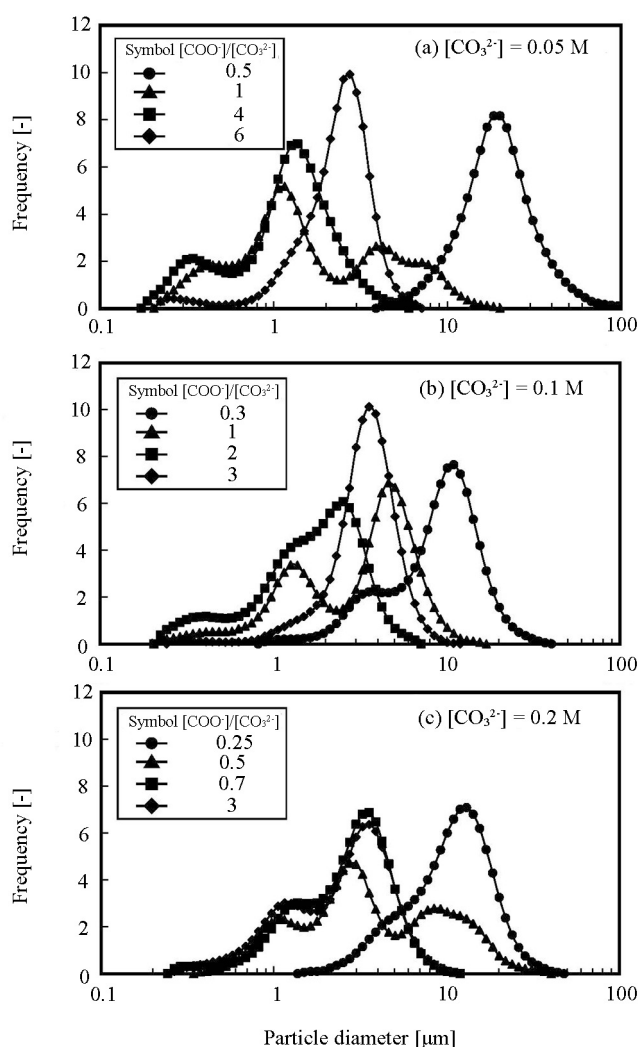

Figure 1. Typical result of particle diameter distribution in the case of using the diluted CaCS solution with adding sodium oxalate as a bicarboxylate. In the case of **(a)** $[CO_3^{2-}]$ = 0.05 M, **(b)** $[CO_3^{2-}]$ = 0.1 M, and **(c)** $[CO_3^{2-}]$ = 0.2 M, Na_2CO_3 was employed in the mixture solution
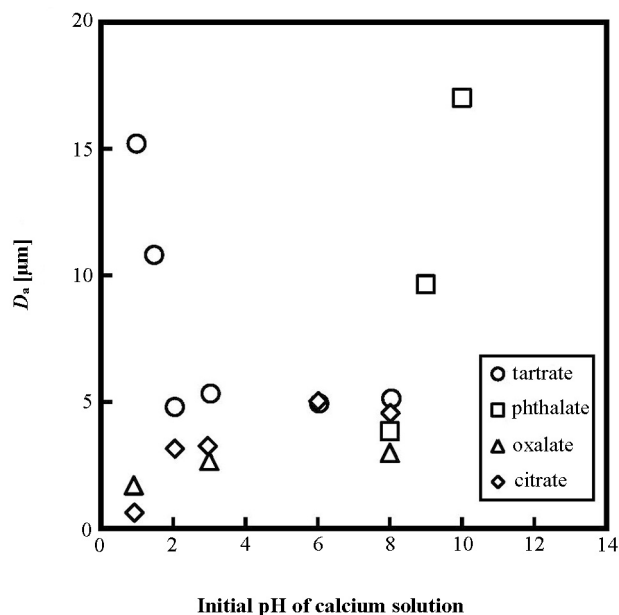
Figure 2. Influence of the initial pH value on the average diameter, D_a, of particles

3.2 *Influence of kinds of carboxylates and the concentrations on the particle size distribution*

Figures 3–6 shows the relationship between the molar ratio ($[COO^-]/[CO_3^{2-}]$) and the average diameter, D_a, of the generated particles for tartrate, phthalate, oxalate, and citrate, respectively. The molar ratio means a ratio of the carboxyl group of carboxylate and CO_3^{2-} in the bicarboxylate/Na_2CO_3 mixed solution ($[COO^-]/[CO_3^{2-}]$). The average diameter, D_a, in the ordinate was calculated from the size distribution of the particles. The concentration of CO_3^{2-} varied from 0.05, 0.1, and 0.2 mol/L which decided the concentration of carboxylate to become desired the molar ratio. The open and solid symbols in Figures 3–6 correspond to that Ca^{2+} included in the calcium solution was derived from reagent ($CaCl_2$) or CaSC solution (shell). As to tartrate and phthalate (Figures 3 and 4), D_a changes with increasing molar ratio to appear as a minimum D_a value. The minimum value of D_a decreased with an increase in the concentration of CO_3^{2-} in the prepared solution. In the case of tartrate (Figure 3), the minimum D_a value increased about 1, 2, and 5 μm. In the case of phthalate (Figure 4), the D_a value increased by about 1, 2, and 3 μm. As to oxalate and citrate (Figures 5 and 6), the definite minima D_a was not observed. In the case of oxalate (Figure 5), in the range over the molar ratio > 1, D_a was mostly about 2 μm. At $[CO_3^{2-}] = 0.2$ M, the experiments in the range over the molar ratio > 1 could not be carried out because of the solubility of sodium oxalate. In the case of citrate, a minimum appeared in the sample made of the calcium solution-derived scallop shell and $[CO_3^{2-}] = 0.2$ M, which was about 4 μm at the molar ratio of 4. The minimum value of D_a was observed in the range of the molar ratio from 2 to 6, which was about 4 μm with $[CO_3^{2-}] = 0.1$ M. The smallest size was observed in the case of adding citrate. These variations of particle size with varying molar ratios might be affected by the competitive binding between carbonated ions and carboxylate ions to calcium ions. The pH values of the 0.1 mol/L CaSC solution and 0.1 mol/L reagent solution ($CaCl_2$) before mixing were 5.92 and 1.49, respectively. The pH values of a typical mixture of sodium carbonate and dicarboxylate were as follows: (1) mixed solution of 0.1 mol/L sodium carbonate and 0.033 mol/L trisodium citrate: pH 10.61; (2) mixed solution of 0.1 mol/L sodium carbonate and 0.1 mol/L trisodium citrate: pH 11.09; (3) mixed solution of 0.1 mol/L sodium carbonate and 0.025 mol/L potassium sodium tartrate tetrahydrate: pH 11.19; (4) mixed solution of 0.1 mol/L sodium carbonate and 0.2 mol/L potassium sodium tartrate tetrahydrate: pH 11.11; (5) mixed solution of 0.1 mol/L sodium carbonate and 0.1 mol/L sodium oxalate: pH 11.58, respectively. In addition, the pH values of the solutions after particle generation using the above mixtures of (1) and (5), and 0.1 mol/L CaSC solution were pH 7.80 and pH 7.29, respectively. The dissociation constant (pK) of tartric acid, citric acid, and oxalic acid have been reported as tartric acid ($pK_1 = 3.03$, $pK_2 = 4.37$)[39], citric acid ($pK_1 = 3.13$, $pK_2 = 4.76$, $pK_3 = 6.4$)[39], and oxalic acid

(pK_1 = 1.25, pK_2 = 3.67)[36], respectively. Judging from the pH values of the solution after particle generation, and the reported dissociation constant values, the added dicarboxylate ions should be perfectly bared, that is, all these ions should charge negatively, so the added dicarboxylate ions could be enough to bind to calcium ion. However, D_a could not become smaller with the increase in the molar ratio. We cannot still give enough reason for this issue.
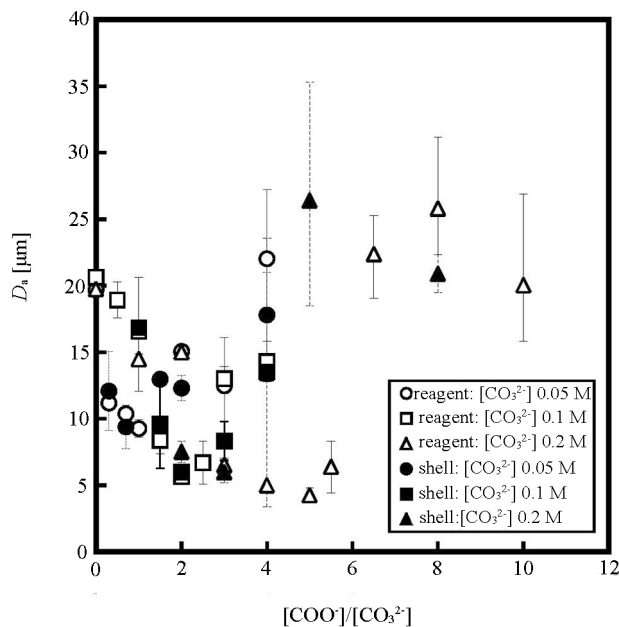

Figure 3. Change in the average diameter of particles by addition of potassium sodium tartrate with varying the molar ratio of carboxyl group and carbonate ion, [COO$^-$]/[CO$_3{}^{2-}$] in the initial solution
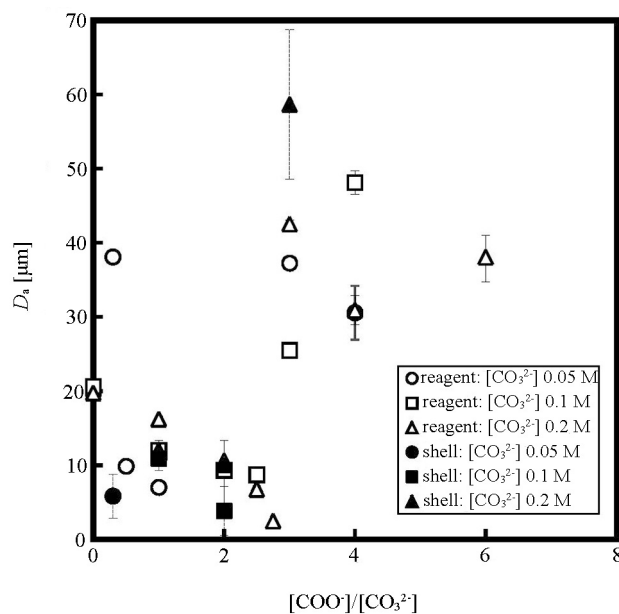
Figure 4. Change in the average diameter of particles by addition of potassium hydrogen phthalate with varying the molar ratio of carboxyl group and carbonate ion, [COO$^-$]/[CO$_3{}^{2-}$] in the initial solution
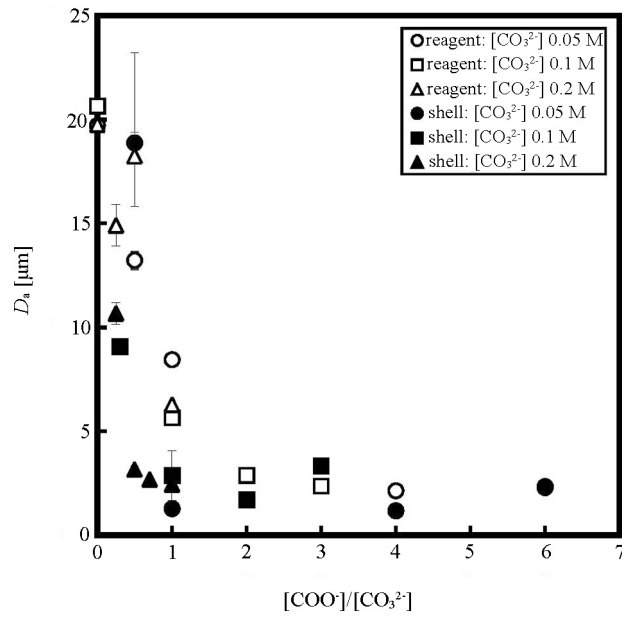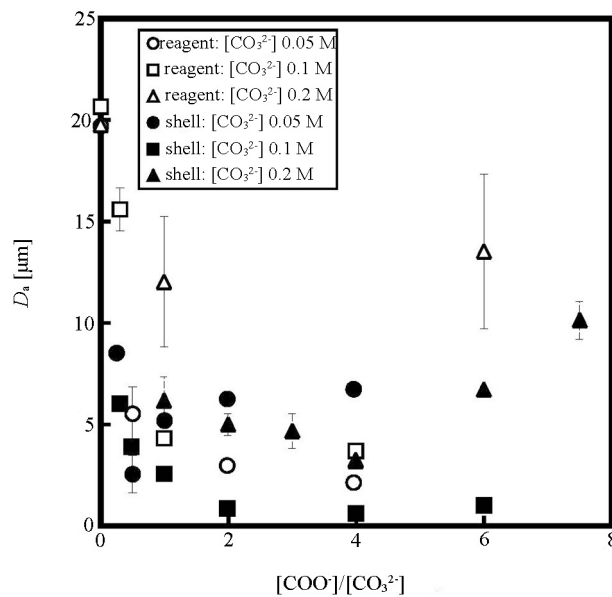
Figure 5. Change in the average diameter of particles by addition of sodium oxalate with varying the molar ratio of carboxyl group and carbonate ion, $[COO^-]/[CO_3^{2-}]$ in the initial solution

Figure 6. Change in the average diameter of particles by addition of sodium citrate with varying the molar ratio of carboxyl group and carbonate ion, $[COO^-]/[CO_3^{2-}]$ in the initial solution

3.3 *Characterization of the generated particles*

Figures 7–10 show the powder X-ray diffraction (XRD) patterns of the $CaCO_3$ particle generated by adding tartrate, phthalate, oxalate, and citrate, respectively. Based on the results of XRD measurement, it was confirmed that there was almost no difference between the $CaCO_3$ particles in the case of using the $CaCl_2$ solution and the diluted CaSC solution. Therefore, the results of XRD measurements in the case of using a $CaCl_2$ solution were not shown. In the case of adding tartrate (Figure 7), two peaks were recognized at 12.4 and 13.3 of 2θ angle value[40], which corresponds to the distinctive

peaks of calcium tartrate tetrahydrate (JCPDF: 00-057-0195) [41]. As the decrease in the ratio of $[COO^-]/[CO_3^{2-}]$, the peaks of calcium tartrate tetrahydrate disappeared (JCPDF: 01-086-4273, 01-083-4604). In the case of adding phthalate (Figure 8), the peaks of vaterite were identified in Figure 8a,b (JCPDF: 00-067-0200, 04-015-9018). On the other hand, in Figure 8a,b, and at $[COO^-]/[CO_3^{2-}] = 2$ (Figure 8c), the peaks of vaterite and calcite were identified. In the case of adding oxalate (Figure 9), several peaks of whewellite (JCPDF: 00-020-0231) were identified. As same as the case of adding phthalate, peaks of vaterite and calcite were identified. In the case of adding citrate, the peaks were mostly identified as calcite (JCPDF: 01-078-4614, 04-008-0788), and some peaks of vaterite were also identified at $[COO^-]/[CO_3^{2-}] = 1.98$ (Figure 10a) and 3.99 (Figure 10b).

On the morphological observation by SEM, in the case of adding tartrate, $CaCO_3$ particles in spherulitic and oval shapes were observed (Figure 11a–c). On the other hand, in the case of adding sodium phthalate, particles in a rectangular shape were also observed (Figure 11f). Spherulitic shapes were also observed on the particles containing vaterite (Figure 12d,e). Sun et al. (2020) reported that they obtained very porous particles (640 m^2/g) when citric acid was added to a system in which calcium oxide was dispersed in methanol and the suspension was aerated with carbon dioxide to produce calcium carbonate [41]. However, in the present system, the addition of citric acid did not produce porous particles. There have been many reports of the spherulitic shape of vaterite particles [21,42,43]. Oiso et al. (2014) investigated the effect of fatty acids addition on the particle properties of mesoporous calcium carbonate and reported that vaterite morph and spherical shape particles were observed by the addition of 15 wt.% butanoic acid [21]. Kirboga and Öner studied the formation of calcium carbonate precipitation in the presence of carboxymethyl inulin and observed spherical particles in the vaterite polymorph [42].
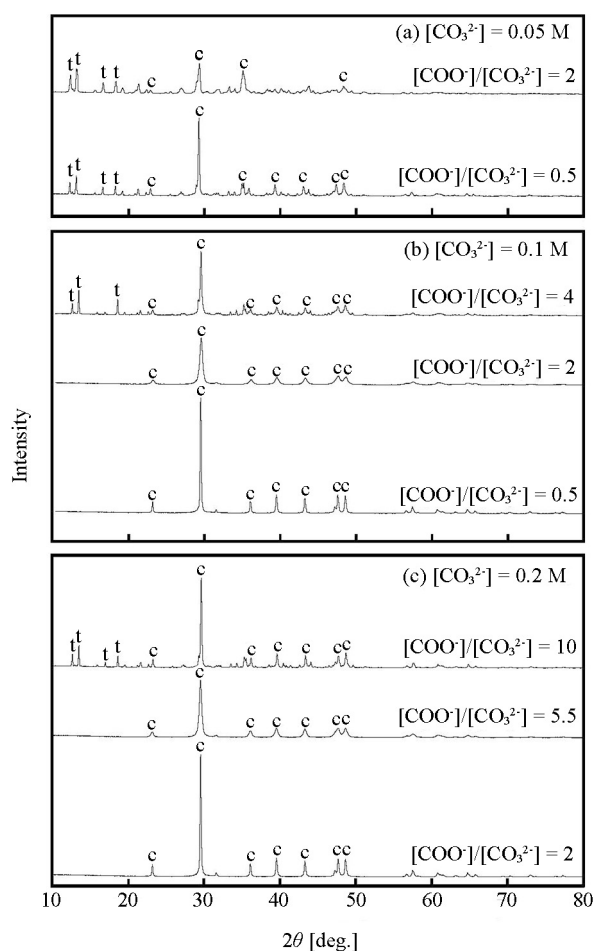

Figure 7. XRD patterns of the particles generated with potassium sodium tartrate. The calcium solution was used CaSC solution. The characters correspond to calcite (c) and calcium tartrate tetra hydrate (t), respectively
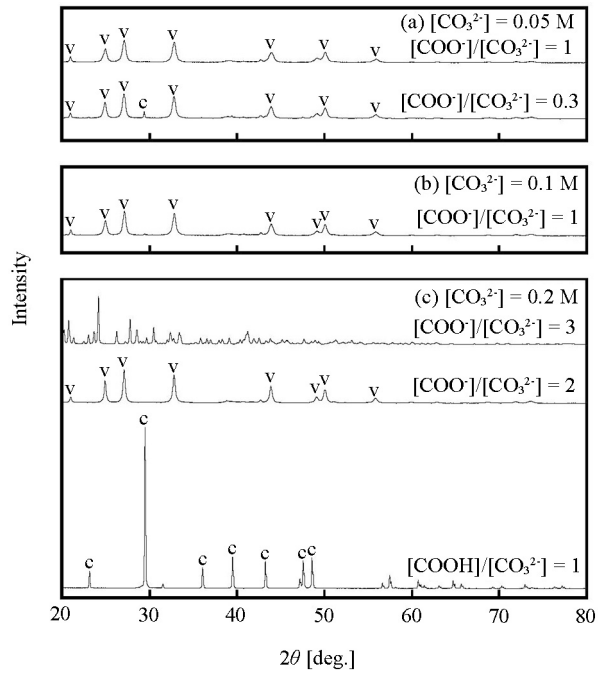
Figure 8. XRD patterns of the particles generated with potassium hyrdogen phthalate. The calcium solution was used CaSC solution. The characters correspond to calcite (c), and vaterite (v), respectively
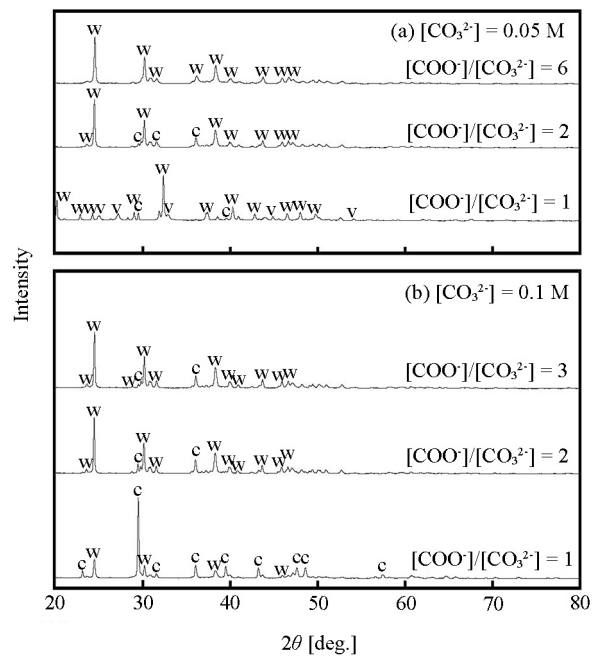

Figure 9. XRD patterns of the particles generated with sodium oxalate. The calcium solution was used CaSC solution. The characters correspond to calcite (c), vaterite (v), and whewellite (w), respectively
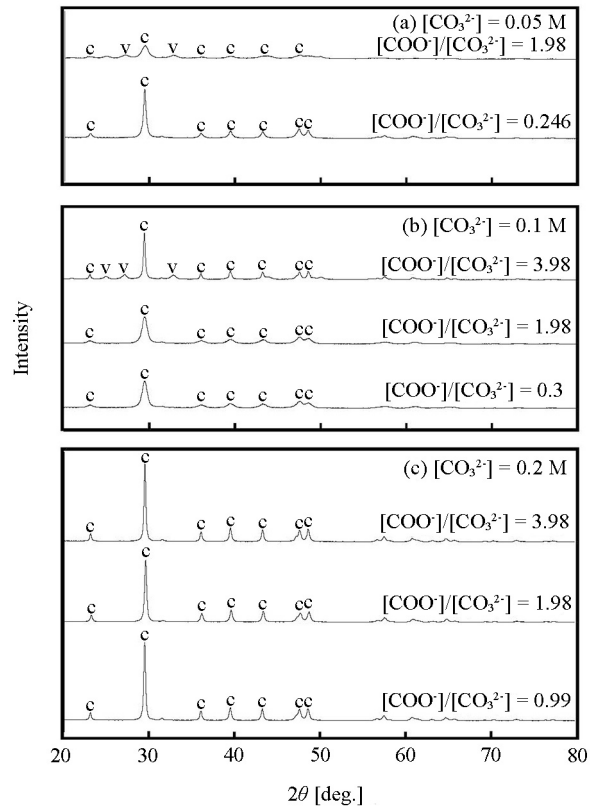
Figure 10. XRD patterns of the particles generated with sodium citrate. The calcium solution was used CaSC solution. The characters correspond to calcite (c) and vaterite (v), respectively
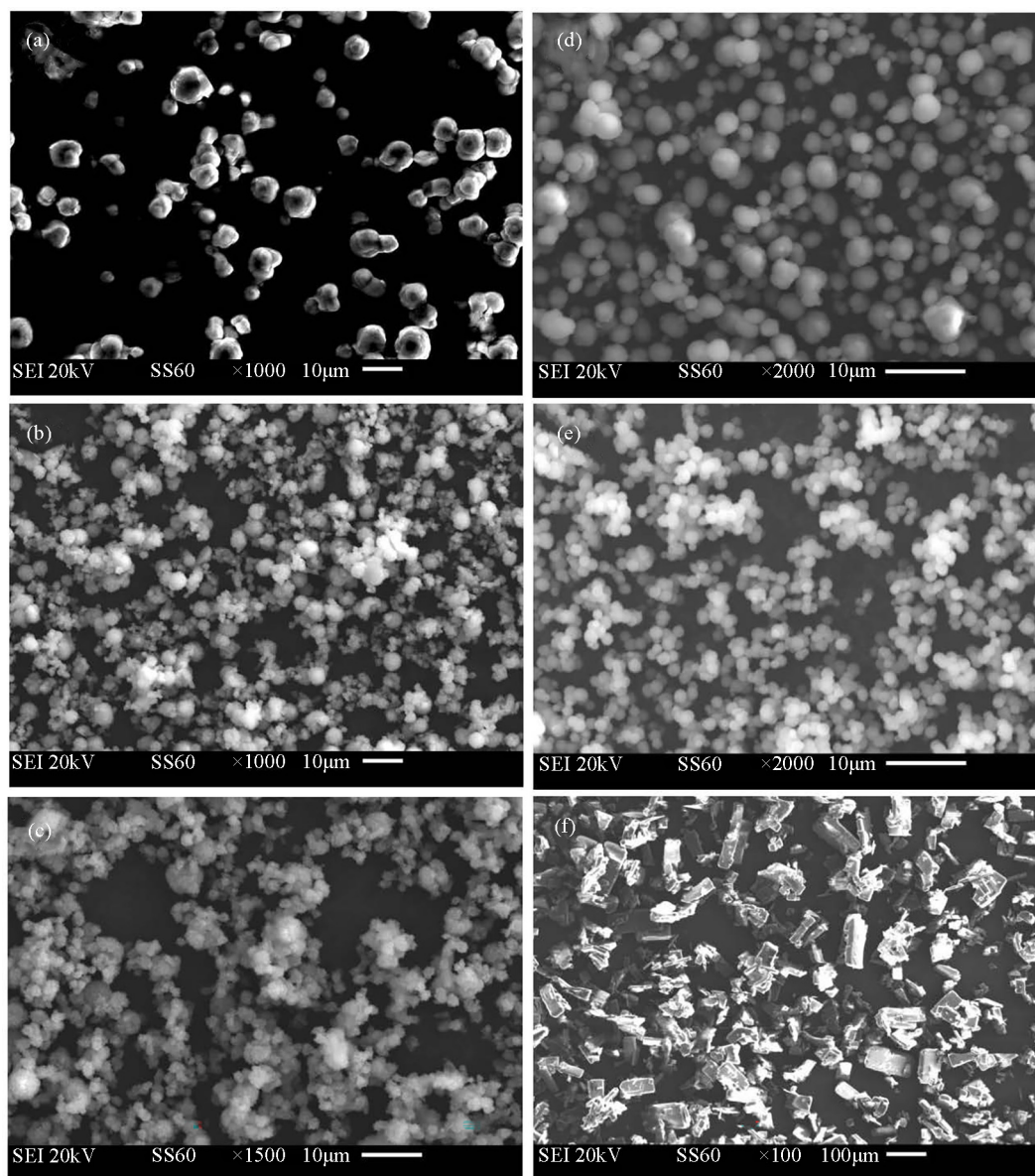
Figure 11. SEM images of the particles generated by adding sodium tartrate (**a**–**c**) and potassium hydrogen phthalate (**d**–**f**). The experimental conditions: (**a**) $[CO_3{}^{2-}]$ 0.05 M, molar ratio 0.3; (**b**) $[CO_3{}^{2-}]$ 0.1 M, molar ratio 4; (**c**) $[CO_3{}^{2-}]$ 0.2 M, molar ratio 5; (**d**) $[CO_3{}^{2-}]$ 0.05 M, molar ratio 1; (**e**) $[CO_3{}^{2-}]$ 0.2 M, molar ratio 2; (**f**) $[CO_3{}^{2-}]$ 0.2 M, molar ratio 3
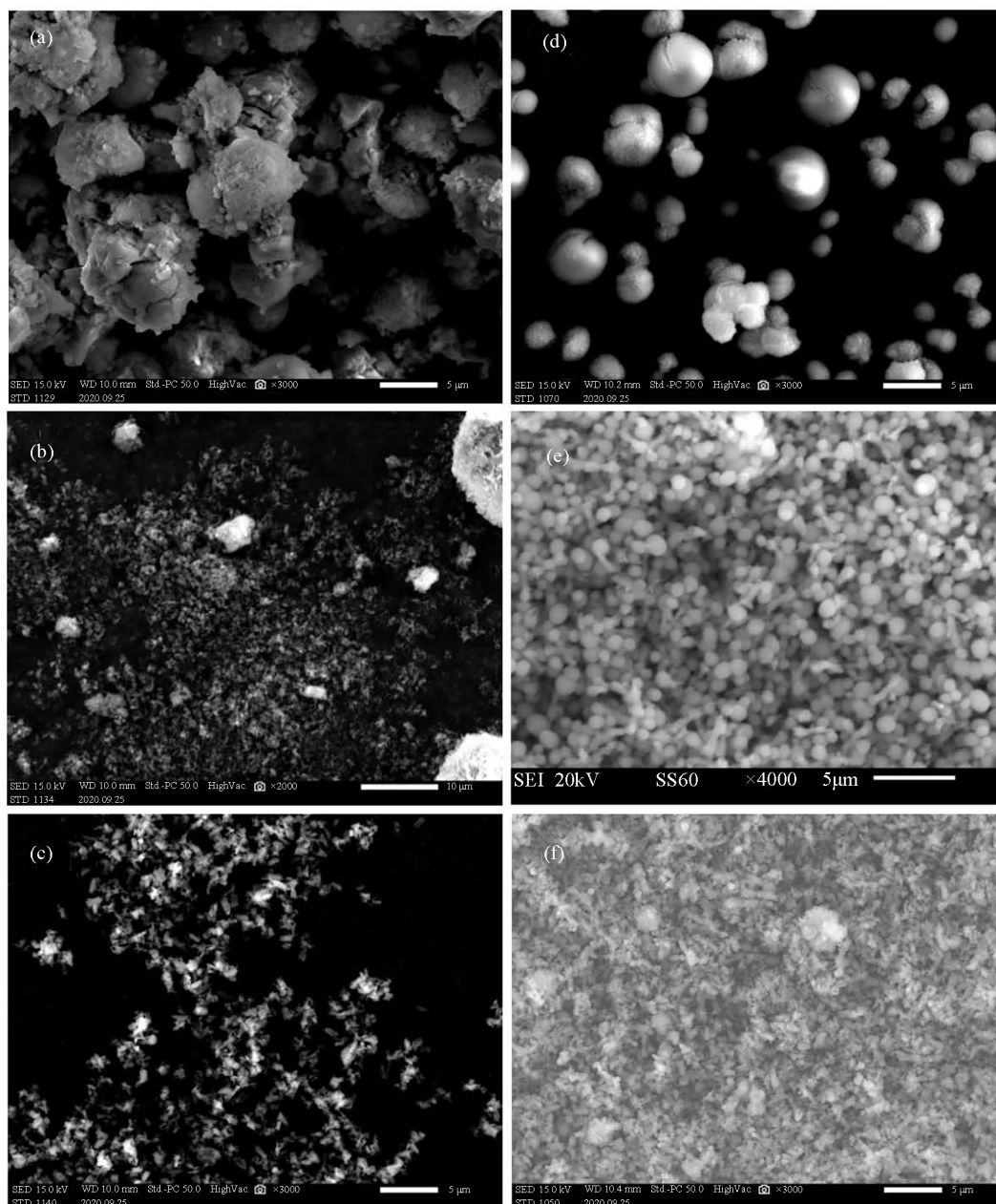
Figure 12. SEM images of the particles generated by adding sodium oxalate (**a**–**c**) and sodium citrate (**d**–**f**). The experimental conditions: (**a**) $[CO_3{}^{2-}]$ 0.1 M, molar ratio 0.3; (**b**) $[CO_3{}^{2-}]$ 0.1 M, molar ratio 1; (**c**) $[CO_3{}^{2-}]$ 0.1 M, molar ratio 2; (**d**) $[CO_3{}^{2-}]$ 0.05 M, molar ratio 1.98; (**e**) $[CO_3{}^{2-}]$ 0.1 M, molar ratio 3.98; (**f**) $[CO_3{}^{2-}]$ 0.2 M, molar ratio 3.98

4. Conclusions

The particle size of the calcium carbonate could be varied by adding divalent or higher carboxylates by precipitation method. This reason might be considered that the carboxylates are assumed to play as the competitive binding partner of the carbonate ions binding to the calcium ions. The polymorph of the calcium carbonate produced was mainly calcite, but calcium tartrate tetrahydrate was observed in the case of adding tartrate, and vaterite polymorph was also observed in the case of adding phthalate or citrate. These regularities of polymorph were not clarified in this study, and further studies on the regularity of polymorph are required in the future. In this study, amorphous calcium carbonate was mainly formed.

The functionality of these materials will be investigated in further study. In addition, We are considering the use of these materials as solid base catalysts or as adsorbents in reaction and separation engineering. In particular, we are interested in how the catalytic performance differs from that of solid base catalysts made simply from calcined shells.

Acknowledgments

Conflict of interest

There is no conflict of interest for this study.

References

[1] Al Omari, M. M. H.; Rashid, I. S.; Qinna, N. A.; Jaber, A. M.; Badwan, A. A. Chapter Two—Calcium Carbonate. *Profiles Drug Subst. Excip. Relat. Methodol.* **2016**, *41*, 31–132.

[2] Mattila, H.-P.; Zevenhoven, R. Chapter Ten—Production of Precipitated Calcium Carbonate from Steel Converter Slag and Other Calcium-Containing Industrial Wastes and Residues. *Adv. Inorg. Chem.* **2014**, *66*, 347–384. https://doi.org/10.1016/B978-0-12-420221-4.00010-X

[3] Galván-Ruiz, M.; Hernández, J.; Baños, L.; Noriega-Montes, J.; Rodríguez-García, M. E. Characterization of Calcium Carbonate, Calcium Oxide, and Calcium Hydroxide as Starting Point to the Improvement of Lime for Their Use in Construction. *J. Mater. Civ. Eng.* **2009**, *21*, 694–698. https://doi.org/10.1061/(asce)0899-1561(2009)21:11(694)

[4] Xiang, L.; Xiang, Y.; Wang, Z.; Jin, Y. Influence of chemical additives on the formation of super-fine calcium carbonate. *Powder Technol.* **2002**, *126*, 129–133. https://doi.org/10.1016/s0032-5910(02)00047-5

[5] Kosaka, Y. Chapter 21- Scallop fisheries and aquaculture in Japan. *Dev. Aquac. Fish. Sci.* **2016**, *40*, 891–936. https://doi.org/10.1016/B978-0-444-62710-0.00021-3

[6] Department of Fisheries and Forestry, Hokkaido Government. *Annual Statistics on Fishery and Aquaculture Production in Hokkaido*; Department of Fisheries and Forestry, Hokkaido Government: Hokkaido, Jaoan, 2020.

[7] Sirisomboonchai, S.; Abuduwayiti, M.; Guan, G.; Samart, C.; Abliz, S.; Hao, X.; Kusakabe, K.; Abudula, A. Biodiesel production from waste cooking oil using calcined scallop shell as catalyst. *Energy Convers. Manag.* **2015**, *95*, 242–247. https://doi.org/10.1016/j.enconman.2015.02.044

[8] Liu, W.; Teng, L.; Rohani, S.; Qin, Z.; Zhao, B.; Xu, C. C.; Ren, S.; Liu, Q.; Liang, B. CO_2 mineral carbonation using industrial solid wastes: A review of recent developments. *Chem. Eng. J.* **2021**, *416*, https://doi.org/10.1016/j.cej.2021.129093

[9] Qin, L.; Gao, X.; Li, Q. Upcycling carbon dioxide to improve mechanical strength of Portland cement. *J. Clean. Prod.* **2018**, *196*, 726–738. https://doi.org/10.1016/j.jclepro.2018.06.120

[10] Feng, B.; Yong, A. K.; An, H. Effect of various factors on the particle size of calcium carbonate formed in a precipitation process. *Mater. Sci. Eng. A* **2007**, *445–446*, 170–179. https://doi.org/10.1016/j.msea.2006.09.010

[11] Jimoh, O. A.; Mahmed, N.; Okoye, P. U.; Ariffin, K. S. Utilization of milk of lime (MOL) originated from carbide lime waste and operating parameters optimization study for potential precipitated calcium carbonate (PCC) production. *Environ. Earth Sci.* **2016**, *75*, 1251. https://doi.org/10.1007/s12665-016-6053-z.

[12] Onimisi, J. A.; Ismail, R.; Ariffin, K. S.; Baharun, N.; Bin Hussin, H. A novel rapid mist spray technique for synthesis of single phase precipitated calcium carbonate using solid-liquid-gas process. *Korean J. Chem. Eng.* **2016**, *33*, 2756–2760. https://doi.org/10.1007/s11814-016-0093-7.

[13] Seo, K.-S.; Han, C.; Wee, J.-H.; Park, J.-K.; Ahn, J.-W. Synthesis of calcium carbonate in a pure ethanol and aqueous ethanol solution as the solvent. *J. Cryst. Growth* **2005**, *276*, 680–687. https://doi.org/10.1016/j.jcrysgro.2004.11.416.

[14] Sand, K. K.; Rodriguez-Blanco, J. D.; Makovicky, E.; Benning, L. G.; Stipp, S. L. S. Crystallization of $CaCO_3$ in Water–Alcohol Mixtures: Spherulitic Growth, Polymorph Stabilization, and Morphology Change. *Cryst. Growth Des.* **2011**, *12*, 842–853. https://doi.org/10.1021/cg2012342.

[15] Trushina, D. B.; Bukreeva, T. V.; Antipina, M. N. Size-Controlled Synthesis of Vaterite Calcium Carbonate by the Mixing Method: Aiming for Nanosized Particles. *Cryst. Growth Des.* **2016**, *16*, 1311–1319. https://doi.org/10.1021/acs.cgd.5b01422.

[16] Kato, T.; Suzuki, T.; Amamiya, T.; Irie, T.; Komiyama, M.; Yui, H. Effects of macromolecules on the crystallization of $CaCO_3$ the Formation of Organic/Inorganic Composites. *Supramol. Sci.* **1998**, *5*, 411–415. https://doi.org/10.1016/s0968-5677(98)00041-8.

[17] Shivkumara, C.; Singh, P.; Gupta, A.; Hegde, M. Synthesis of vaterite $CaCO_3$ by direct precipitation using glycine and l-alanine as directing agents. *Mater. Res. Bull.* **2006**, *41*, 1455–1460. https://doi.org/10.1016/j.materresbull.2006.01.026.

[18] Kim, J.-H.; Song, S. M.; Kim, J. M.; Kim, W. S.; Kim, I. H. $CaCO_3$ crystallization with feeding of aspartic acid. *Korean J. Chem. Eng.* **2010**, *27*, 1532–1537. https://doi.org/10.1007/s11814-010-0245-0.

[19] Saraya, M. E.-S. I. Effect of L (+) ascorbic acid and monosodium glutamate concentration on the morphology of calcium carbonate. *J. Solid State Chem.* **2015**, *231*, 114–122. https://doi.org/10.1016/j.jssc.2015.08.020.

[20] Karar, A.; Naamoune, F.; Kahoul, A.; Belattar, N. Inhibitory effect of glutamic acid on the scale formation process using electrochemical methods. *Environ. Technol.* **2016**, *37*, 1996–2002. https://doi.org/10.1080/09593330.2016.1139629.

[21] Oiso, T.; Yamanaka, S.; Fujimoto, T.; Ohira, Y.; Kuga, Y. Effect of Fatty Acids Addition on the Particle Properties of Mesoporous Calcium Carbonate. *J. Soc. Powder Technol. Jpn.* **2014**, *51*, 816–822. https://doi.org/10.4164/sptj.51.816.

[22] Jiang, J.; Xu, D.; Zhang, Y.; Zhu, S.; Gan, X.; Liu, J. From nano-cubic particle to micro-spindle aggregation: The control of long chain fatty acid on the morphology of calcium carbonate. *Powder Technol.* **2015**, *270*, 387–392. https://doi.org/10.1016/j.powtec.2014.10.047.

[23] Zhao, Y.; Du, W.; Sun, L.; Yu, L.; Jiao, J.; Wang, R. Facile synthesis of calcium carbonate with an absolutely pure crystal form using 1-butyl-3-methylimidazolium dodecyl sulfate as the modifier. *Colloid Polym. Sci.* **2013**, *291*, 2191–2202. https://doi.org/10.1007/s00396-013-2960-7.

[24] Yang, X.; Meng, H.; Li, T.; Shi, L.; Li, Y.; Xu, G. $CaCO_3$ crystallization in HPCHS/CTAB mixed solutions. *Powder Technol.* **2014**, *256*, 272–278. https://doi.org/10.1016/j.powtec.2014.02.020.

[25] Page, M. G.; Nassif, N.; Börner, H. G.; Antonietti, M.; Cölfen, H. Mesoporous Calcite by Polymer Templating. *Cryst. Growth Des.* **2008**, *8*, 1792–1794. https://doi.org/10.1021/cg700899s.

[26] Zhang, X.; Yan, F.; Guo, C.; Li, F.; Chen, G.; Huang, Z.; Yuan, G. Preparation and structure of calcium peroxide-templated porous calcium carbonate crystals. *Cryst. Res. Technol.* **2011**, *46*, 664–668. https://doi.org/10.1002/crat.201100115.

[27] Yan, F.-W.; Guo, C.-Y.; Zhang, X.-H.; Yuan, G.-Q. Synthesis and characterization of spherical porous calcium carbonate with ordered secondary structures in the presence of polymer with double hydrophilic ionic moieties. *CrystEngComm* **2011**, *14*, 1554–1560. https://doi.org/10.1039/c1ce05897e.

[28] Choi, K.-M.; Kuroda, K. Polymorph Control of Calcium Carbonate on the Surface of Mesoporous Silica. *Cryst. Growth Des.* **2012**, *12*, 887–893. https://doi.org/10.1021/cg201314k.

[29] Kirboga, S.; Öner, M. Application of experimental design for the precipitation of calcium carbonate in the presence of biopolymer. *Powder Technol.* **2013**, *249*, 95–104. https://doi.org/10.1016/j.powtec.2013.07.015.

[30] Yu, H.-D.; Tee, S. Y.; Han, M.-Y. Preparation of porosity-controlled calcium carbonate by thermal decomposition of volume content-variable calcium carboxylate derivatives. *Chem. Commun.* **2012**, *49*, 4229–4231. https://doi.org/10.1039/c2cc35339c.

[31] Gopi, S.; Subramanian, V.; Palanisamy, K. Aragonite–calcite–vaterite: A temperature influenced sequential polymorphic transformation of $CaCO_3$ in the presence of DTPA. *Mater. Res. Bull.* **2013**, *48*, 1906–1912. https://doi.org/10.1016/j.materresbull.2013.01.048.

[32] Palanisamy, K.; Subramanian, V. $CaCO_3$ scale deposition on copper metal surface; effect of morphology, size and area of contact under the influence of EDTA. *Powder Technol.* **2016**, *294*, 221–225. https://doi.org/10.1016/j.powtec.2016.02.036.

[33] Sun, S.; Gebauer, D.; Cölfen, H. A general strategy for colloidal stable ultrasmall amorphous mineral clusters in organic solvents. *Chem. Sci.* **2016**, *8*, 1400–1405. https://doi.org/10.1039/c6sc02333a.

[34] Jia, X.; Kayitmazer, A. B.; Ahmad, A.; Ramzan, N.; Li, Y.; Xu, Y.; Sun, S. Polyacids for producing colloidally stable amorphous calcium carbonate clusters in water. *J. Appl. Polym. Sci.* **2021**, *139*, 51899. https://doi.org/10.1002/app.51899.

[35] Tobler, D. J.; Rodriguez-Blanco, J. D.; Dideriksen, K.; Bovet, N.; Sand, K. K.; Stipp, S. L. S. Citrate Effects on Amorphous Calcium Carbonate (ACC) Structure, Stability, and Crystallization. *Adv. Funct. Mater.* **2015**, *25*, 3081–3090. https://doi.org/10.1002/adfm.201500400.

[36] Miyashita, M.; Yamada, E.; Kawano, M. Influence of low–molecular–weight dicarboxylic acids on the formation of calcium carbonate minerals in solutions with Mg^{2+} ions. *J. Miner. Pet. Sci.* **2018**, *113*, 207–217. https://doi.org/10.2465/jmps.180406.

[37] Henderson, G. E.; Murray, B. J.; McGrath, K. M. Controlled variation of calcite morphology using simple carboxylic acids. *J. Cryst. Growth* **2008**, *310*, 4190–4198. https://doi.org/10.1016/j.jcrysgro.2008.07.002.

[38] Maruyama, H.; Seki, H. Esterification of tripalmitin using calcined scallop shell as a heterogeneous basic catalyst. *Asia-Pacific J. Chem. Eng.* **2022**, *18*. https://doi.org/10.1002/apj.2870.

[39] Lu, Q.; Li, M.; Zhang, L.; Gan, C. Regulation of Calcite Morphology by Low-Molecular-Weight Organic Acids: Alcohol Hydroxyl and Carboxyl Matters. *Cryst. Res. Technol.* **2023**. https://doi.org/10.1002/crat.202300113.

[40] Pradyumnan, P. P.; Shini, C. Growth characterization and etching studies of calcium tartrate single crystal grown using tamarind extract. *Indian J. Pure Appl. Phys.* **2009**, *47*, 199–205. http://nopr.niscpr.res.in/handle/123456789/3443.

[41] Sun, R.; Tai, C.-W.; Strømme, M.; Cheung, O. The effects of additives on the porosity and stability of amorphous calcium carbonate. *Microporous Mesoporous Mater.* **2020**, *292*. https://doi.org/10.1016/j.micromeso.2019.109736.

[42] Kirboga, S.; Öner, M. Application of experimental design for the precipitation of calcium carbonate in the presence of biopolymer. *Powder Technol.* **2013**, *249*, 95–104. https://doi.org/10.1016/j.powtec.2013.07.015.

[43] Song, X.; Liu, H.; Wang, J.; Cao, Y.; Luo, X. A study of the effects of NH_4^+ on the fast precipitation of vaterite $CaCO_3$ formed from steamed ammonia liquid waste and K_2CO_3/Na_2CO_3. *CrystEngComm* **2021**, *23*, 4284–4300.